Photoelectron Spectroscopy Of Rare Gas Dimers

ATANU GHOSH (CY09C005)
NABADYUTI BARMAN (CY 09C022)
M PAVAN KUMAR (CY10D044)
E UMESH BABU (CY10D056)
T V RAMA MOHAN (CY10DO57)

Photoelectron spectroscopy of rare gas dimers

1.LCAO of rare gas dimers give the following configuration

$$\cdots(\sigma_g ns)^2(\sigma_u ns)^2(\sigma_g np)^2(\pi_u np)^4(\pi_g np)^4(\sigma_u np)^2.$$

n=3,4,5 for Ar,Kr,Xe
respectively

2.The ionic states observed in He1 region are

$$\cdots(\sigma_g ns)^2(\sigma_u ns)^2(\sigma_g np)^2(\pi_u np)^4(\pi_g np)^4(\sigma_u np)^1\ A\,^2\Sigma_u^+,$$

$$\cdots(\sigma_g ns)^2(\sigma_u ns)^2(\sigma_g np)^2(\pi_u np)^4(\pi_g np)^3(\sigma_u np)^2\ B\,^2\Pi_g,$$

$$\cdots(\sigma_g ns)^2(\sigma_u ns)^2(\sigma_g np)^2(\pi_u np)^3(\pi_g np)^4(\sigma_u np)^2\ C\,^2\Pi_u^+,$$

$$\cdots(\sigma_g ns)^2(\sigma_u ns)^2(\sigma_g np)^1(\pi_u np)^4(\pi_g np)^4(\sigma_u np)^2\ D\,^2\Sigma_g^+$$

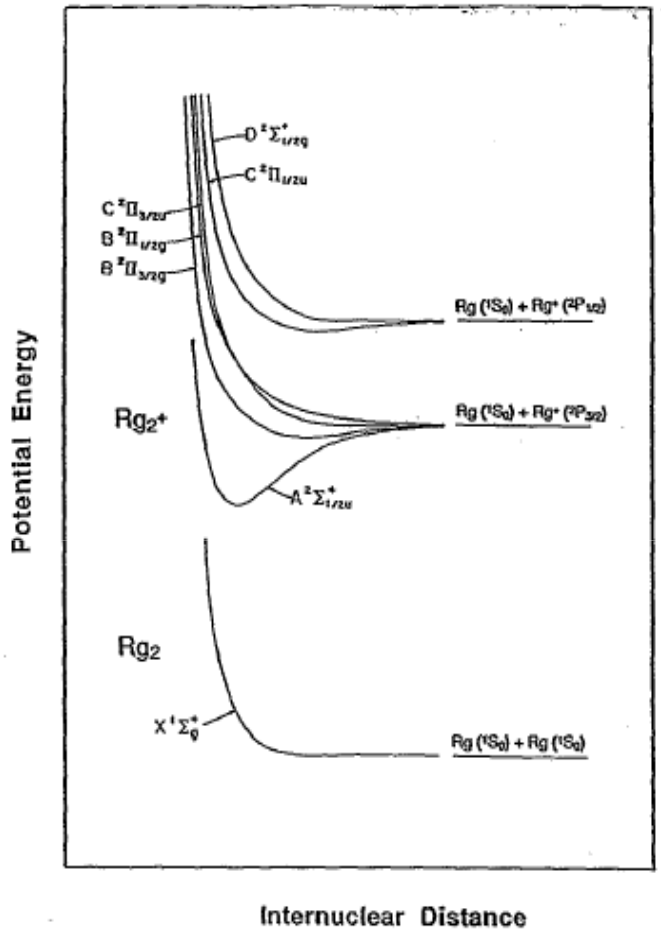

FIG. 1. Schematic potential energy curves of the neutral and the first six ionic states of the rare gas dimers.

T. Pradeep, B. Niu, D.A. Shirley, J. Chem. Phys., Vol. 98, No. 7, 1993

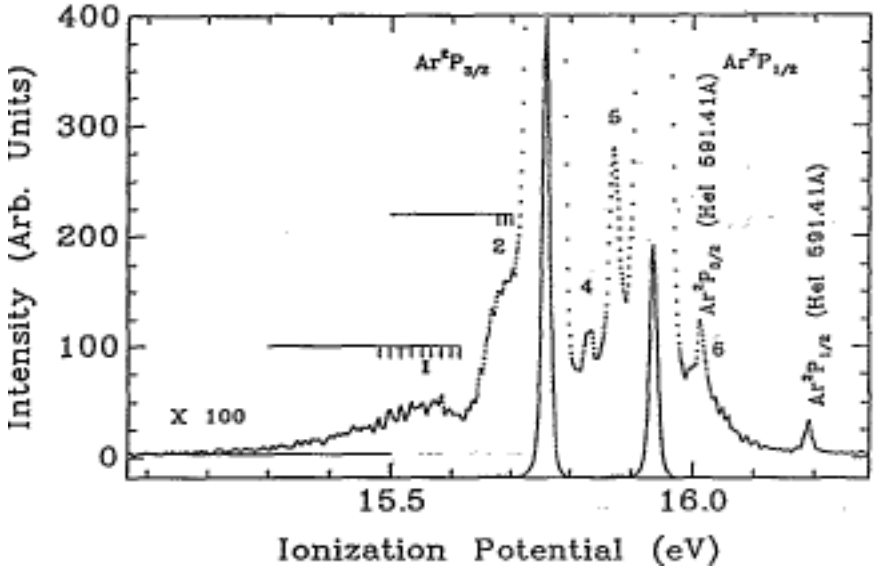

FIG. 2. He I photoelectron spectrum of a mixture of Ar and Ar2 at a stagnation pressure of 280 Torr and at a nozzle temperature of 80 K with an instrumental resolution of 13 meV as. The spectrum has been truncated to enhance the dimer features which are 100 times weaker than the atomic *2P312 peak.*. The vibrational fine structures on features 1 and 2 are marked with vertical lines. A gradual rise in the intensity above the background is seen beginning at 15.138±0.OO3 eV, which is identified as the appearance energy of the dimer.

FIG. 3. A semilog plot of the data presented in Fig. 2 near the dimer features. The feature labeled 3 corresponds to the C *2II3/2g state.*

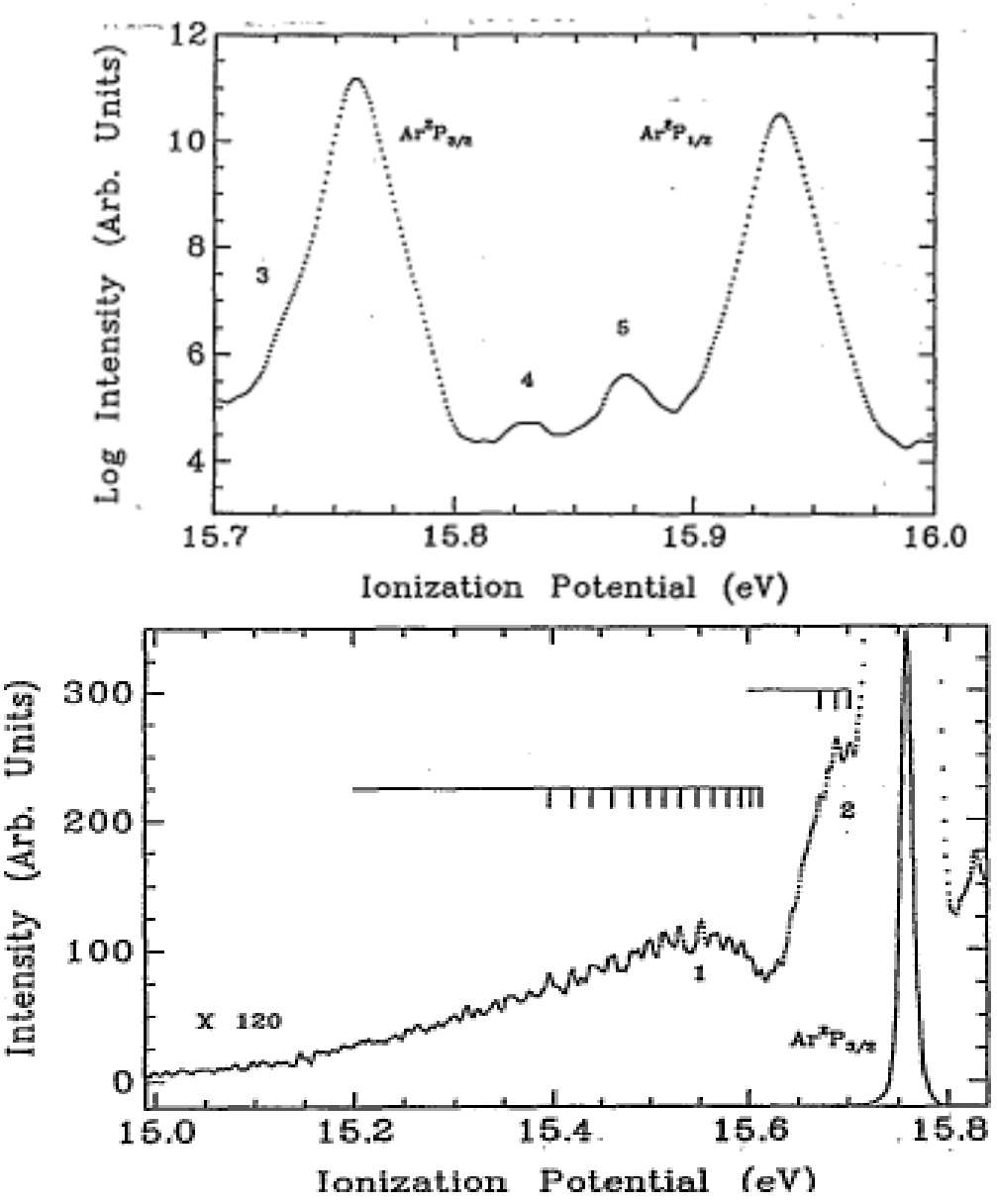

FIG. 4. He I photoelectron spectrum of a mix.ture of Ar and Ar2 at a stagnation pressure of 150 Torr and at a nozzle temperature of 80 K.

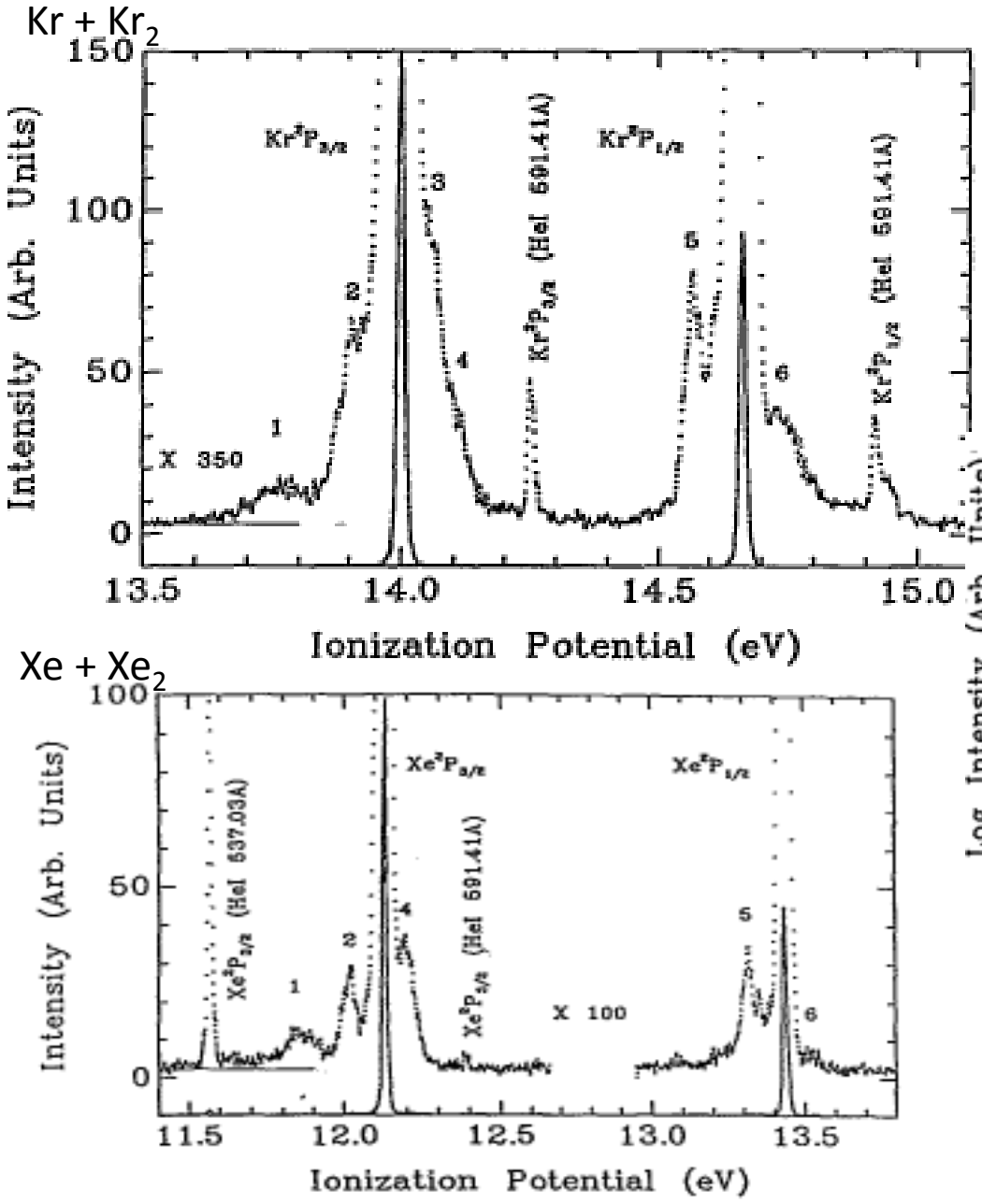

FIG. 6. The He I photoelectron spectrum of a mixture of Xe and X~ at a nozzle stagnation pressure of 820 Torr and at a nozzle temperature of 300 K

FIG. 5. The He I photoelectron spectrum of a mixture of Kr and Kr2 at a nozzle stagnation pressure of 800 Torr and at a nozzle temperature of 300 K.

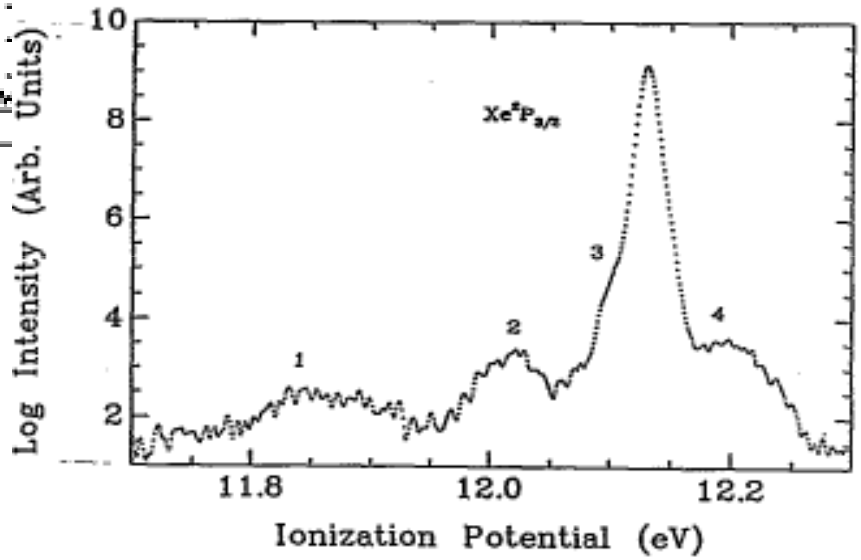

FIG. 7. A semilog plot of the data presented in Fig. 5 in the Xe *2P3/2* region.

Table: Ionisation potential and dissociation energies[a] of the ionic states of dimmers observed in the He 1 energy region.

Peak	State	Adiabatic I.E. (eV) ±0.003			Vertical I.E.(eV)			Dissociation energy (eV) ±0.003		
		Ar_2	Kr_2	Xe_2	Ar_2	Kr_2	Xe_2	Ar_2	Kr_2	Xe_2
1	$A^2\Sigma^+_{1\2u}$	..b	…b	….b	15.548 ±0.003	13.773 ±0.003	11.845 ±0.015	…….	…….	…….
2	$B^2\Pi_{3\2g}$	15.630	13.831	11.97	15.689 ±0.001	13.907 ±0.001	12.02 ± 0.001	0.139	0.184	0.185
3	$C^2\Pi_{3\2u}$	15.708	…….	……..	15.734 ±0.003	14.055 ±0.003	12.089 ± 0.001	0.061	c	……
4	$B^2\Pi_{1\2g}$	…….	……..	……..	15.829 ±0.001	14.117 ±.003	12.198 ±0.001	c	c	c
5	$C^2\Pi_{1\2u}$	15.847	14.530	13.27	15.871 ±0.001	14.566 ±0.001	13.316 ±0.001	0.001	0.151	0.19
6	$D^2\Sigma^+_{1\2g}$	15.934	14.653	……..	15.998 ±0.003	14.728 ±0.003	13.518 ±0.003	0.013	0.028	…….

[a] The experimental values correspond to D_o not D_e

[b] The adiabatic I.E. is not observed due to poor Frank-condon factors

[c] repulsive states

Resonance Enhanced Multiphoton Ionization Spectroscopy (REMPI)

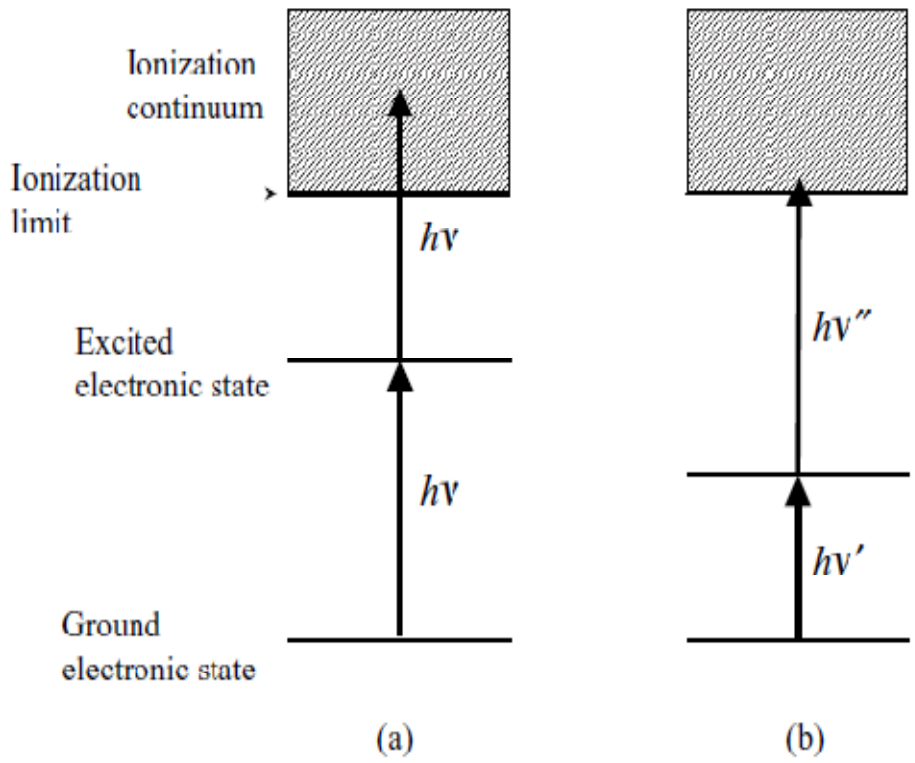

Dispersive Photoelectron spectroscopy of the ungerade Rydberg states of Xe_2 near Xe^* (6p, 5d)

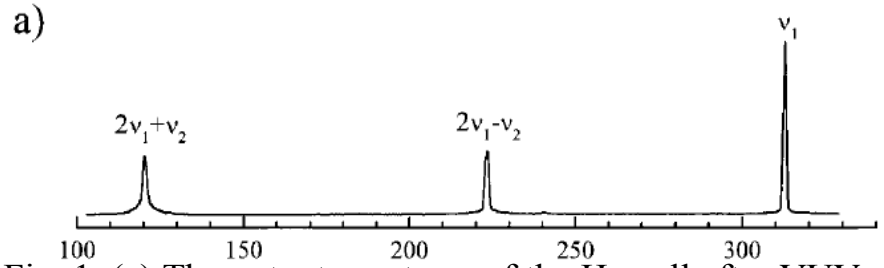

Fig. 1. (a) The output spectrum of the Hg cell after VUV generation. The fundamental visible beam at ϑ_2 is not observed due to the detection range of the solar-blind photomultiplier tube.

$$\mathrm{Xe}_2(v''=0) \overset{h\nu_{\mathrm{ex}}}{\rightarrow} \mathrm{Xe}_2^*(v') \overset{h\nu_{\mathrm{ion}}}{\rightarrow} \mathrm{Xe}_2^+(v^+) + \mathrm{e}^-$$

$$\mathrm{KE} = h\nu_{\mathrm{ex}} + h\nu_{\mathrm{ion}} - [A_{\mathrm{IP}} + G(v^+)]$$

$$\mathrm{Xe}_2(v''=0) \overset{h\nu_{\mathrm{ex}}}{\rightarrow} \mathrm{Xe}_2^*(v') \rightarrow \mathrm{Xe} + \mathrm{Xe}^* \overset{h\nu_{\mathrm{ion}}}{\rightarrow} \mathrm{Xe} + \mathrm{Xe}^+ + \mathrm{e}^-$$

$$\mathrm{KE} = h\nu^*(\mathrm{Xe}) + h\nu_{\mathrm{ion}} - \mathrm{IP}(\mathrm{Xe}^+),$$

D. M. Mao et al., chemical physics 257, 2000, 253 - 261

Band System near Xe^* $6p[1/2]_0$

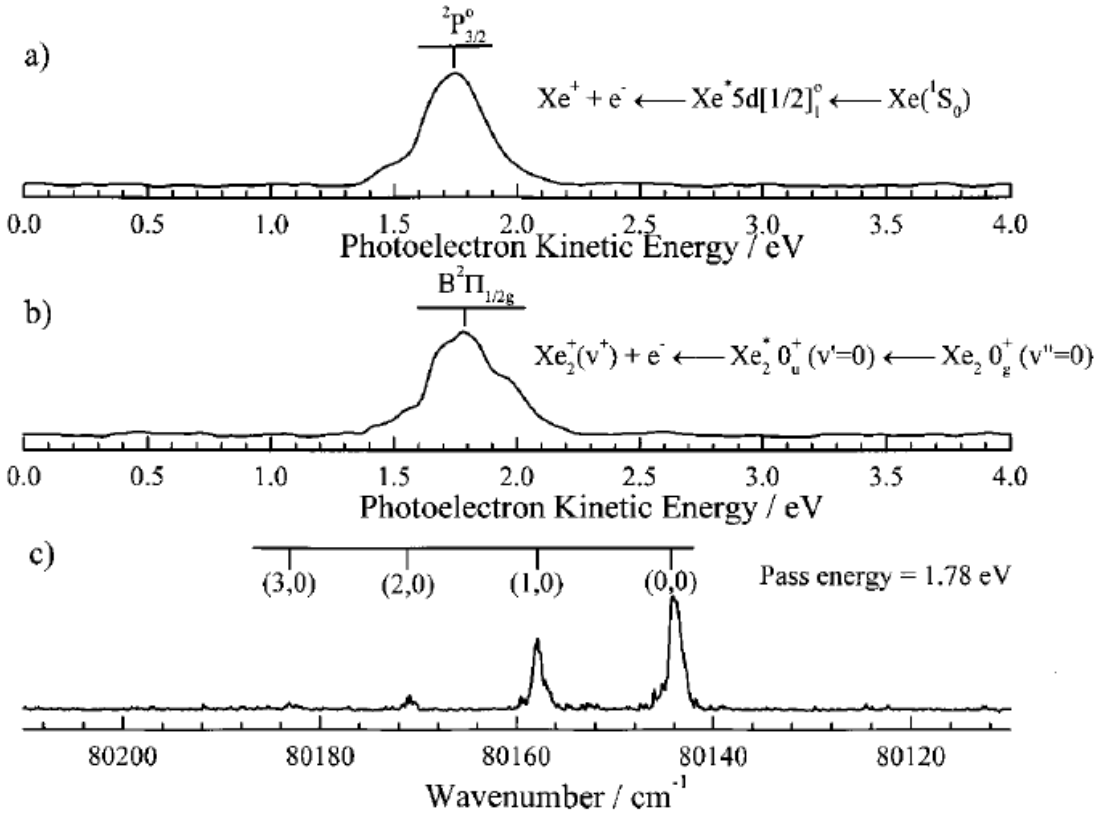

Fig. 2. (a) PE spectrum obtained by exciting the Xe^* $5d[1/2]^0_1 \leftarrow Xe(^1S_0)$ atomic transition at 79986.55 cm^{-1}; (b) PE spectrum obtained by exciting the Xe_2^* $0_u^+(v'=0) \leftarrow Xe_2$ $0_g^+(v''=0)$ transition in the vicinity of Xe^* $6p[1/2]_0$ and (c) CIS spectrum of Xe_2 in the vicinity of Xe^* $6p[1/2]_0$ obtained by setting the pass energy of the photoelectron spectrometer to 1.78 eV and scanning the VUV laser.

Band system Near Xe^* $5d[5/2]_3{}^0$

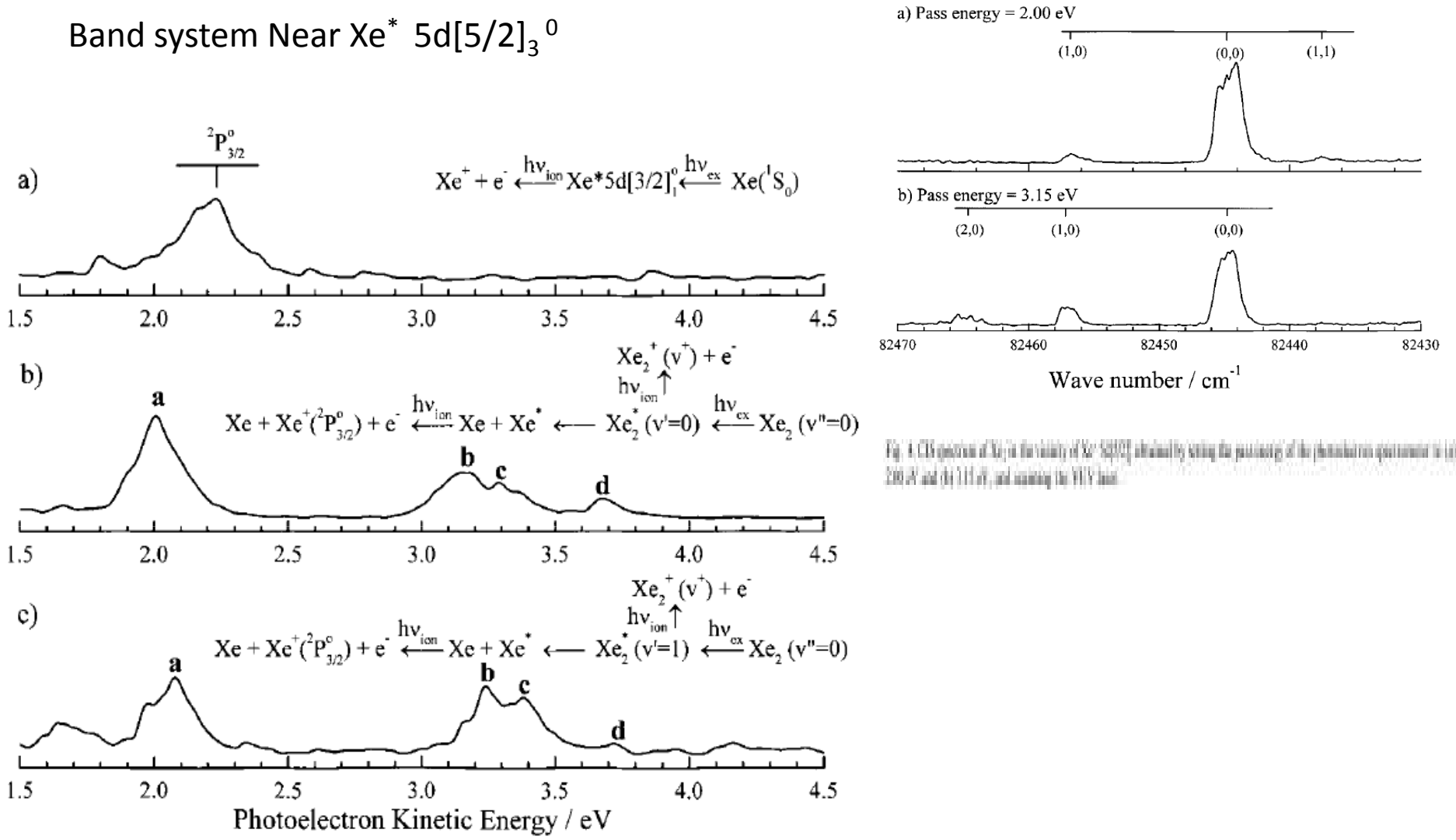

Fig. 3. (a) PE spectrum obtained by exciting the Xe^* $5d[3/2]^v_1 \leftarrow Xe(^1S_0)$ atomic transition at 83 899.99 cm^{-1}; (b) PE spectrum of the Xe_2^* $0^+_u(v'=0) \leftarrow Xe_2$ $0^+_g(v''=0)$ transition in the vicinity of Xe^* 5d $[5/2]^0_3$ and (c) PE spectrum of the Xe_2^* $0^+_u(v'=1) \leftarrow Xe_2$ $0^+_g(v''=0)$ transition in the vicinity of Xe^* 5d $[5/2]^0_3$.

Band system Near Xe^* $5d[3/2]_1^0$

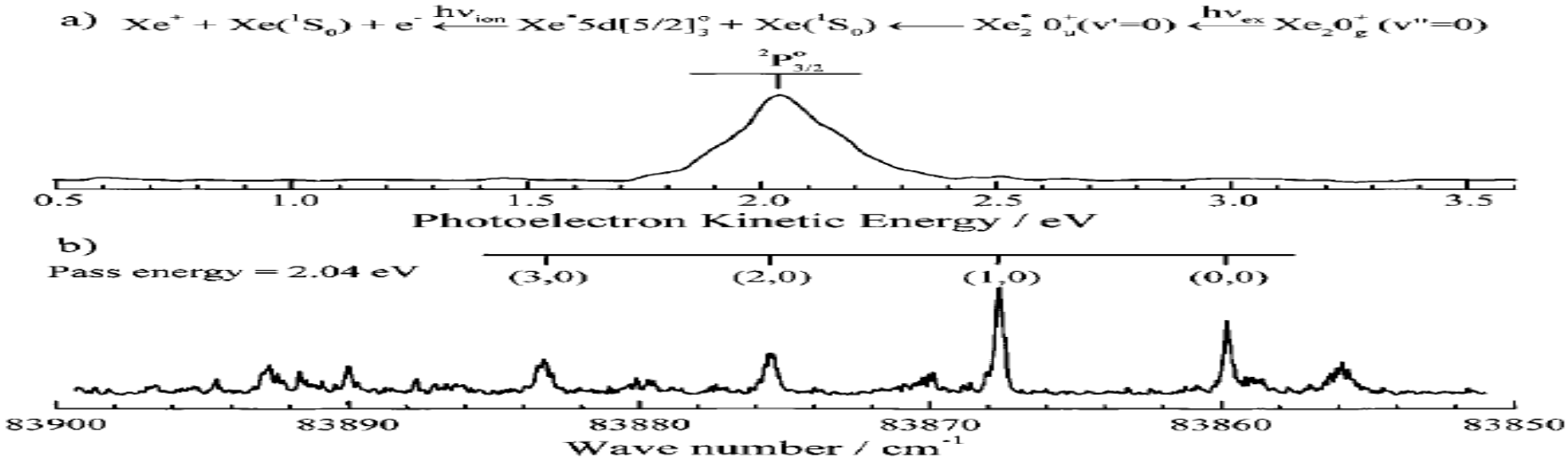

Fig. 5. (a) PE spectrum of the $Xe_2^* \, 0_u^+(v' = 0) \leftarrow Xe_2 \, 0_g^+(v'' = 0)$ transition in the vicinity of Xe^* $5d[3/2]_1^0$; (b) CIS spectrum of Xe_2 in the vicinity of Xe^* $5d[3/2]_1^0$ obtained by setting the pass energy of the photoelectron spectrometer to 2.04 eV and scanning the VUV laser.

Transitions, photoelectric kinetic energies, KE, ionization photon, ν_{ion}, and dominant core assignments for Rydberg states of Xe_2 that dissociate to $Xe(^1S_0)+Xe^*(6p,5d)$

Asymptote	Transition	Wave number (cm^{-1})	ν_{ion}	KE (eV)	Dominant core assignment
$Xe + Xe^*$ $6p[1/2]_0$	$0_u^+(v' = 0) \leftarrow 0_g^+(v'' = 0)$	80 143	ν_1	1.78	$Xe_2^+(B^2\Pi_{1/2g})$
$Xe + Xe^*$ $5d[5/2]_3^0$	$0_u^+(v' = 0) \leftarrow 0_g^+(v'' = 0)$	82 444	ν_1	2.00	$Xe_2^+(C^2\Pi_{3/2u})$
			$2\nu_1 - \nu_2$	3.15	$Xe^+(^2P_{3/2}^0)^a$
			$2\nu_1 - \nu_2$	3.31	$Xe^+(^2P_{3/2}^0)^b$
			$2\nu_1 - \nu_2$	3.66	$Xe_2^+(C^2\Pi_{3/2u})$
$Xe + Xe^*$ $5d[3/2]_1^0$	$0_u^+(v' = 0) \leftarrow 0_g^+(v'' = 0)$	83 760	ν_1	2.04	$Xe^+(^2P_{3/2}^0)^c$
	$0_u^+(v' = 1) \leftarrow 0_g^+(v'' = 0)$	83 793	ν_1	2.00	$Xe^+(^2P_{3/2}^0)^c$
	$0_u^+(v' = 2) \leftarrow 0_g^+(v'' = 0)$	83 827	ν_1	2.04	$Xe^+(^2P_{3/2}^0)^c$
	$0_u^+(v' = 3) \leftarrow 0_g^+(v'' = 0)$	83 861	ν_1	2.02	$Xe^+(^2P_{3/2}^0)^c$

[a] Predissociation to Xe^* $6p[5/2]_2$.
[b] Predissociation to Xe^* $6p[1/2]_0$.
[c] Predissociation to Xe^* $5d[5/2]_3^0$.

INNER SHELL SPECTROSCOPY AND EXCHANGE INTERACTION OF RYDBERG ELECTRONS BOUND BY SINGLY AND DOUBLY CHARGED Kr & Xe ATOMS IN SMALL CLUSTERS(<15>)

Two types of interactions in clusters of rare gas

1) Induced Polarization (XPS)
2) Exchange interaction(XAS& RAS)

There is three types of process occurring →

1) Core photo ionization
2) Excitation to Rydberg state
3) Resonant Auger decay.

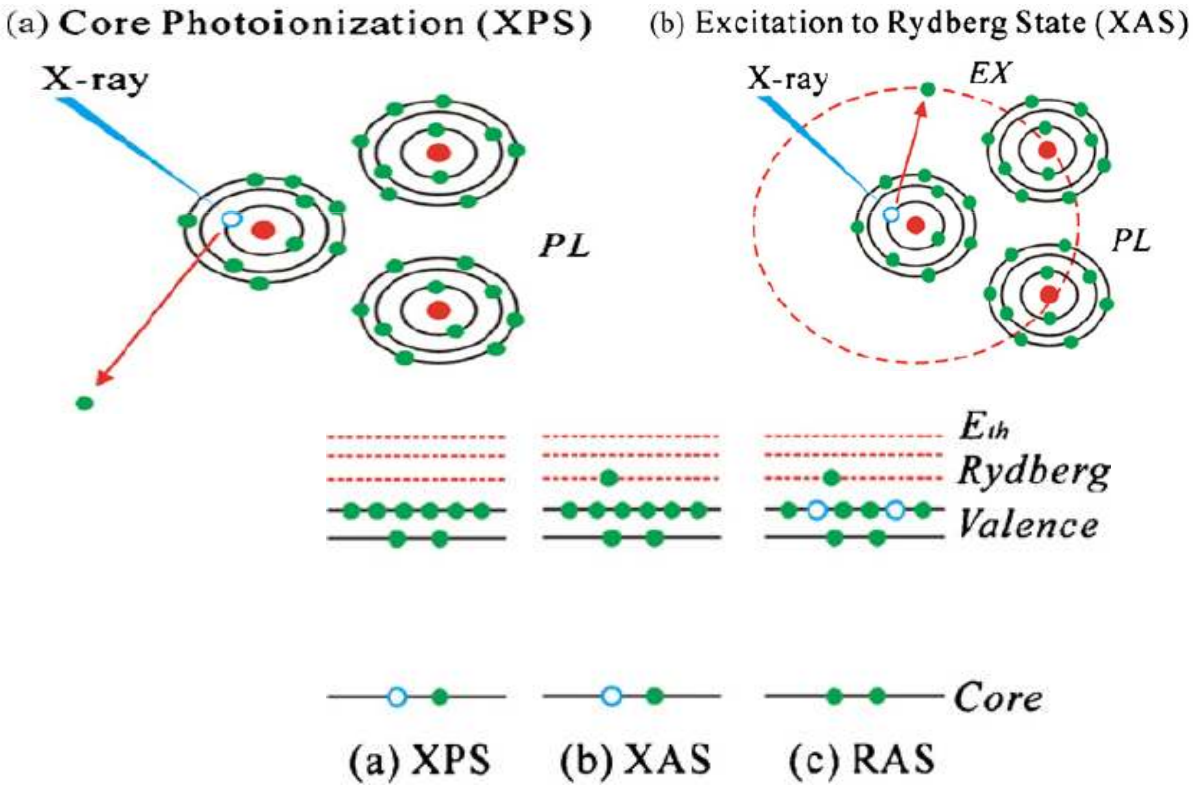

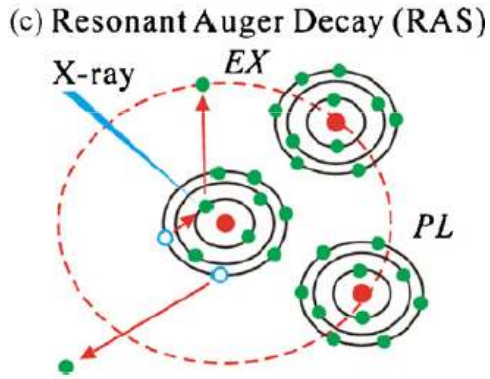

M.Nagasaka et al., journal of electron spectroscopy and related phenomena 183, 2011, 29 - 35

XPS STUDY

Assumptions about cluster from XPS study:

• Fcc like close packing but with 13 atoms of 15 atoms of the clusters having corner Edge face and bulk sites.

• Icosahedron structure with 13 atoms.

•The peak intensity ratios of corner , edge, bulk & face are different for each types of packing.

• The induced polarization is inversely proportional with van der waals radius.

The equation for induced polarization is

$$E_{iPL}(Z) = \frac{-\alpha Z^2}{2(4\pi\varepsilon_0)^2 r^4}$$

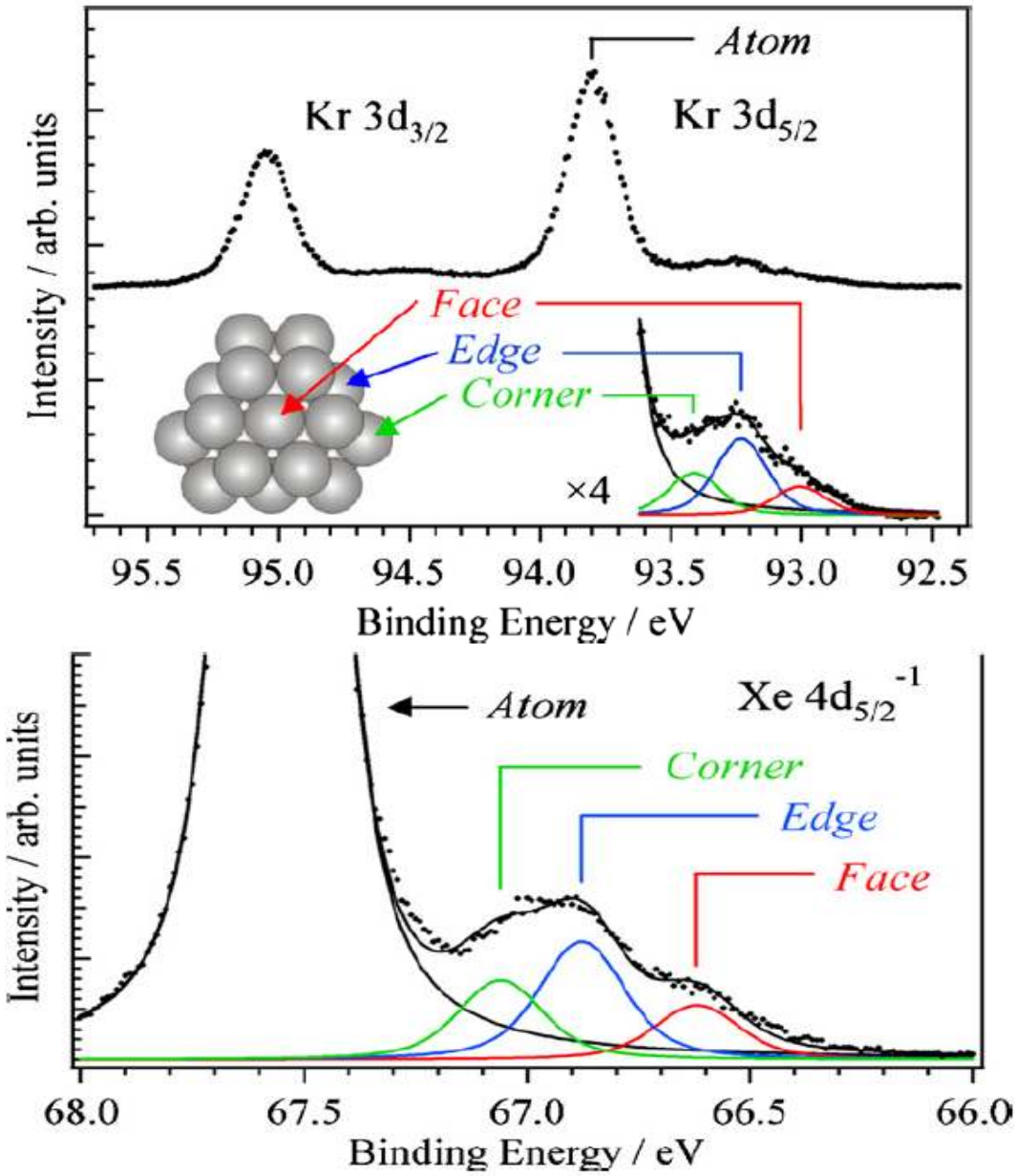
Atom
Kr 3d3/2
Kr 3d5/2
Face
Edge
Corner
×4
Intensity / arb. units
95.5
95.0
94.5
94.0
93.5
93.0
92.5
Binding Energy / eV

Atom
Xe 4d5/2-1
Corner
Edge
Face
Intensity / arb. units
68.0
67.5
67.0
66.5
66.0
Binding Energy / eV

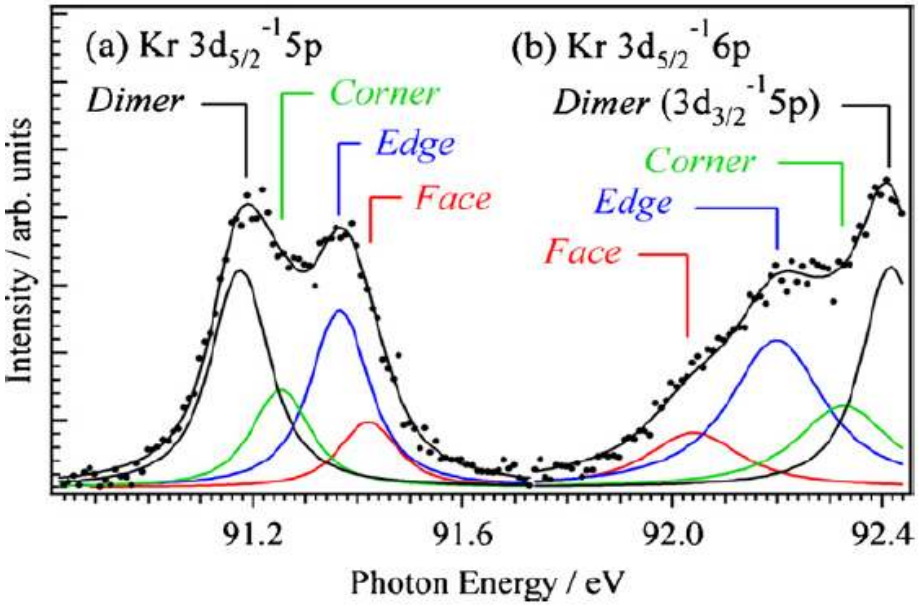

Fig. 4. Surface-site resolved Kr $3d_{5/2}^{-1}5p$ and $3d_{5/2}^{-1}6p$ XAS spectra of Kr clusters with $\langle N \rangle = 15$, measured in the dimer ion (Kr_2^+) yields. The cluster 5p Rydberg states are blueshifted from the dimer one whereas the 6p states are redshifted.

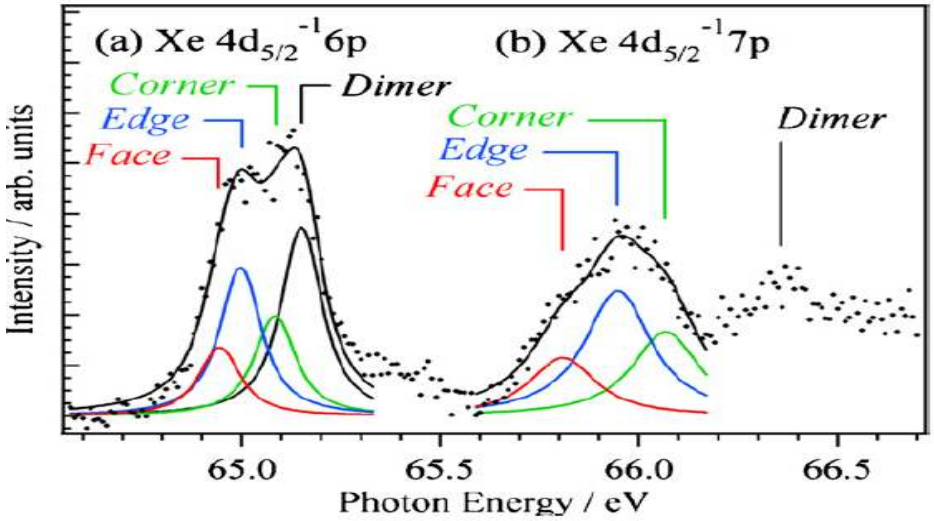

Fig. 5. Surface-site resolved Xe $4d_{5/2}^{-1}6p$ and $4d_{5/2}^{-1}7p$ XAS spectra of Xe clusters with N = 15, measured in the dimer ion (Xe^{2+}) yields. The cluster 6p and 7p Rydberg states are both redshifted from the dimer one.

XAS & RAS study

•XAS spectra in dimer kr^{2+} is decomposed with dimers and three different suface sites in the energy region

The exchange energy interaction E_{EX} (+1) dependent on respective Rydberg states can be evaluated

According g to the following equation

$$E_{EX}(+1) = \Delta E_{XAS} - E_{iPL}(+1)$$

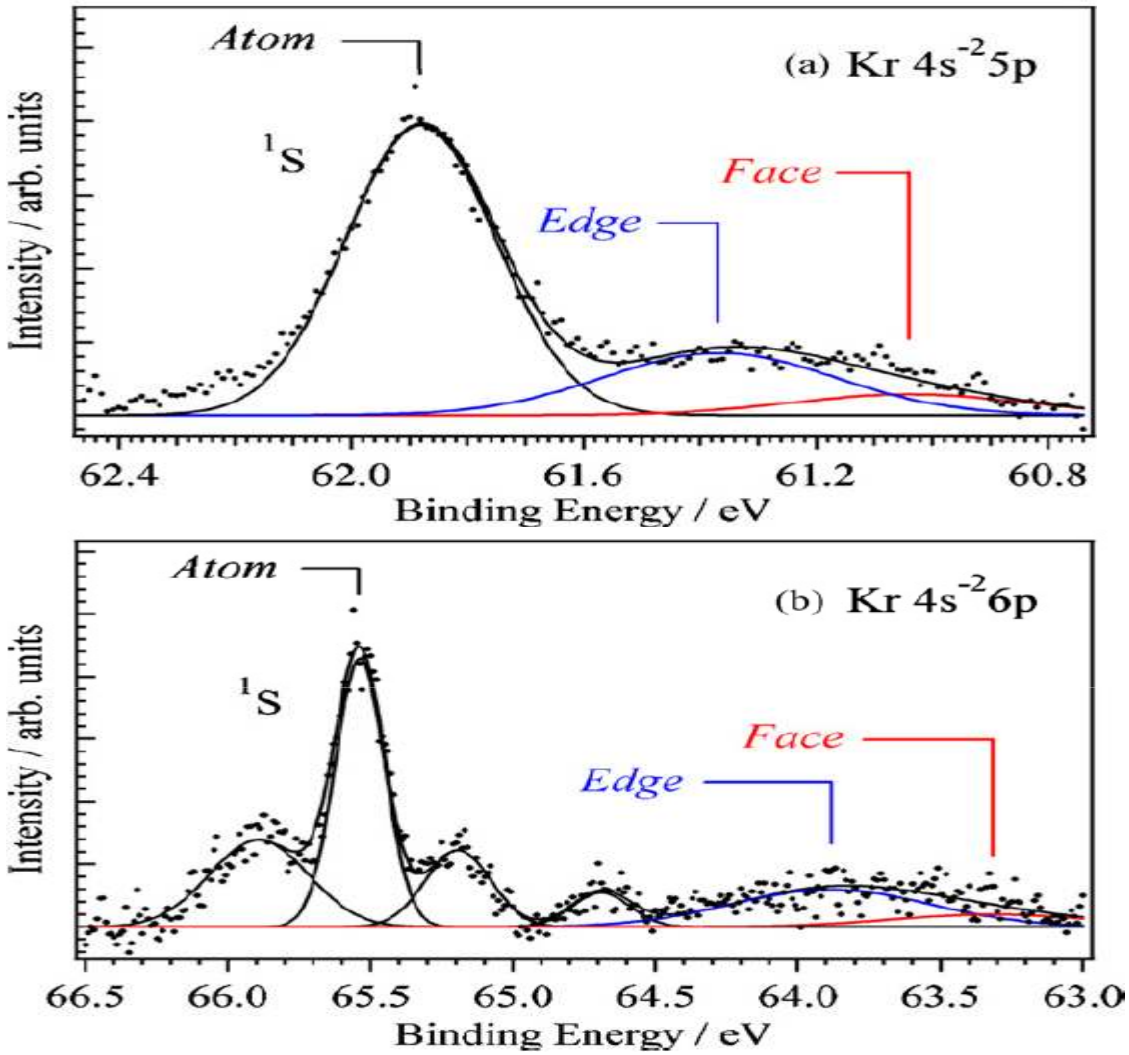

Fig. 6. Surface-site resolved Kr $4s^{-2}$ 5p and $4s^{-2}$ 6p spectator-like RAS spectra of Kr clusters with N = 15, following the resonant excitation (h = 91.37 eV) to the edge site in the $3d_{5/2}{}^{-1}5p$ Rydberg state. Both the cluster 5p and the 6p Rydberg states are redshifted from the atomic one.

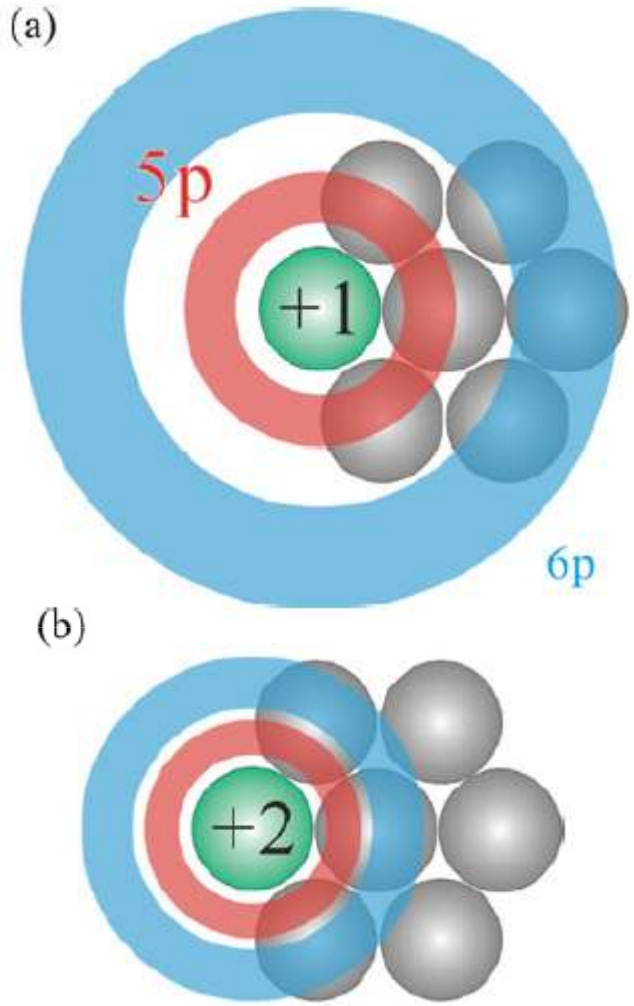

Fig. 7. Conceptional Kr 5p and 6p Rydberg orbitals bound by the singly and doubly ionized states.

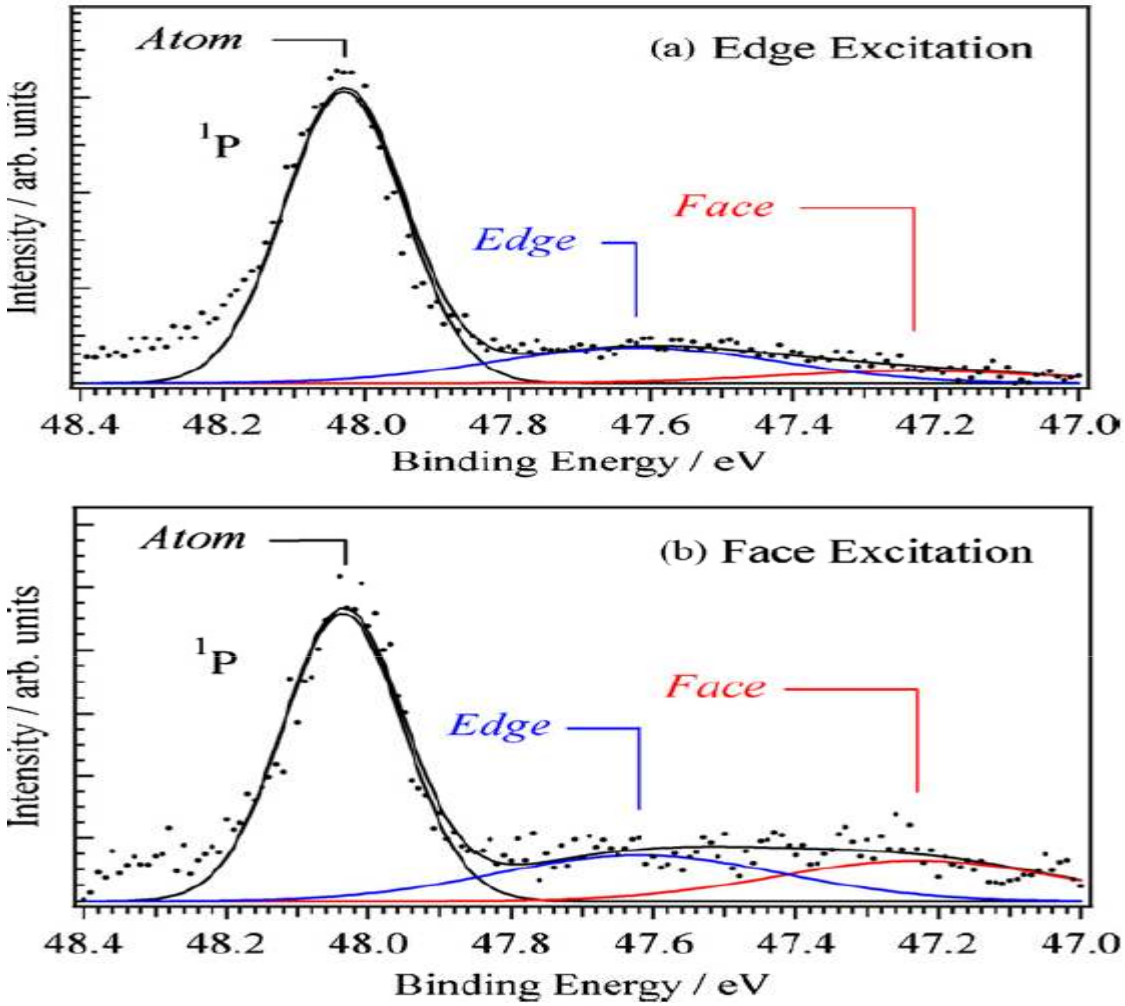

Fig. 8. Surface-site resolved Kr $4s^{-1}\,4p^{-1}\,5p$ spectator-like RAS spectra of Kr clusters with N = 15, following the resonant excitations to (a) the edge site in the $3d_{5/2}{}^{-1}6p$ Rydberg state (h = 92.20 eV) and (b) the face site in the $3d_{5/2}{}^{-1}6p$ Rydberg state (92.04 eV).


Thank you!